Ab Initio Quantum Mechanical Study of the Structures and Energies for the Pseudorotation of 5′-Dehydroxy Analogues of 2′-Deoxyribose and Ribose Sugars

Ken A. Brameld and William A. Goddard III*

Contribution from the Materials and Process Simulation Center, Beckman Institute (139-74), Division of Chemistry and Chemical Engineering, California Institute of Technology, Pasadena, California 91125

Received August 20, 1998. Revised Manuscript Received November 25, 1998

Abstract: We have used ab initio quantum mechanical (QM) methods to determine the potential energy of pseudorotation for 3,4-dihydroxy-5-methyl-2-(1-pyrollyl)tetrahydrofuran and 4-hydroxy-5-methyl-2-(1-pyrollyl)-tetrahydrofuran, close analogues of 2′-deoxyribose and ribose sugars. The pyrrole is a substitute for the naturally occurring nucleic acid bases: adenine, thymine, guanine, cytosine, and uracil. At the highest calculation level (LMP2/cc-pVTZ(-f)//HF/6-31G**) for 2′-deoxyribose, we find the C2′-endo conformation is the global minimum. The C3′-endo conformation is a local minimum 0.6 kcal/mol higher in energy, and an eastern barrier of 1.6 kcal/mol separates the two minima. Pseudorotation energies of ribose are quite complex and are strongly affected by local orientations of the 2′ and 3′ hydroxyl groups. When the hydroxyl groups are allowed to assume any conformation, the global minimum remains the C2′-endo conformation. The eastern barrier increases slightly to 1.8 kcal/mol, and the C3′-endo local minimum lies 0.6 kcal/mol above the global minimum. Constraining the torsion angle of the C3′ hydroxyl group to −146°, as is found in RNA polymers, results in the C3′-endo conformation becoming the only energy minimum with a C2′-endo conformation 1.9 kcal/mol higher in energy. Bond angles within the pentofuranose ring are correlated to the pseudorotational phase, as is observed by X-ray crystallography and is predicted by pseudorotation theory. Finally, a force field for use in molecular mechanics and dynamics simulations is presented which reproduces the QM potential energies for the 2′-deoxyribose and ribose sugars.

Introduction

Ribose and 2′-deoxyribose sugars are the basic subunits which differentiate RNA and DNA, respectively. The conformations of these substituted pentofuranose sugars is of critical importance to the global structure of nucleic acids and has been the subject of considerable theoretical and experimental study. A fundamental concept governing the conformations of five-membered rings was first formulated to describe the interconversion of conformations of cyclopentane through "pseudorotation." [1] For cyclopentane, the lowest energy conformation will have one atom positioned out of the plane, defined by the remaining four atoms of the ring. Through pseudorotation, ring conformations having different out-of-plane atoms may interconvert without traversing a high-energy planar structure.

For cyclopentane, this process of pseudorotation has little or no energy barrier, resulting in essentially "free" ring pucker motion.[2−4] In the case of tetrahydrofuran (THF) and the more complex 2′-deoxyribose and ribose sugars, there are barriers to interconversion stemming from the O4′ oxygen in the ring and the exocyclic hydroxyl groups.[3,5] NMR experiments offer a straightforward approach to determine the relative energies of low-energy pucker states.[6−21] However, the magnitude of the energy barrier between these stable conformations has escaped experimental measurement, except for purine ribosides.[6] The

* Author to whom all correspondence should be addressed.

(1) Kilpatrick, J. E.; Pitzer, K. S.; Spitzer, R. *J. Am. Chem. Soc.* **1947**, *69*, 2483−2488.
(2) Cremer, D.; Pople, J. A. *J. Am. Chem. Soc.* **1975**, *97*, 1358.
(3) Saenger, W. *Principles of Nucleic Acid Structure*; Springer-Verlag: New York, 1984.
(4) Cui, W. L.; Li, F. B.; Allinger, N. L. *J. Am. Chem. Soc.* **1993**, *115*, 2943−2951.
(5) Olson, W. K. *J. Am. Chem. Soc.* **1982**, *104*, 278−286.
(6) Roder, O.; Ludemann, H.-D.; von Goldammer, E. *Eur. J. Biochem.* **1975**, *53*, 517−525.
(7) Olson, W. K.; Sussman, J. L. *J. Am. Chem. Soc.* **1982**, *104*, 270−278.
(8) de Leeuw, F. A. A. M.; Vanbeuzekom, A. A.; Altona, C. *J. Comput. Chem.* **1983**, *4*, 438−448.
(9) de Leeuw, F. A. A. M.; Altona, C. *J. Comput. Chem.* **1983**, *4*, 428−437.
(10) de Leeuw, F. A. A. M.; Haasnoot, C. A. G.; Altona, C. *J. Am. Chem. Soc.* **1984**, *106*, 2299−2306.
(11) de Leeuw, F. A. A. M.; Vankampen, P. N.; Altona, C.; Diez, E.; Esteban, A. L. *J. Mol. Struct. (THEOCHEM)* **1984**, *125*, 67−88.
(12) Diez, E.; Esteban, A. L.; Bermejo, F. J.; Altona, C.; de Leeuw, F. A. A. M. *J. Mol. Struct. (THEOCHEM)* **1984**, *125*, 49−65.
(13) Chuprina, V. P.; Nerdal, W.; Sletten, E.; Poltev, V. I.; Fedoroff, O. Y. *J. Biomol. Struct. Dyn.* **1993**, *11*, 671−683.
(14) Plavec, J.; Tong, W. M.; Chattopadhyaya, J. *J. Am. Chem. Soc.* **1993**, *115*, 9734−9746.
(15) Emsley, L.; Dwyer, T. J.; Spielmann, H. P.; Wemmer, D. E. *J. Am. Chem. Soc.* **1993**, *115*, 7765−7771.
(16) Carmichael, I.; Chipman, D. M.; Podlasek, C. A.; Serianni, A. S. *J. Am. Chem. Soc.* **1993**, *115*, 10863−10870.
(17) Oleary, D. J.; Kishi, Y. *J. Org. Chem.* **1994**, *59*, 6629−6636.
(18) Thibaudeau, C.; Plavec, J.; Chattopadhyaya, J. *J. Am. Chem. Soc.* **1994**, *116*, 8033−8037.
(19) Plavec, J.; Thibaudeau, C.; Chattopadhyaya, J. *Pure Appl. Chem.* **1996**, *68*, 2137−2144.
(20) Lam, S. L.; Auyeung, S. C. F. *J. Biomol. Struct. Dyn.* **1996**, *13*, 803−814.
(21) Luyten, I.; Thibaudeau, C.; Sandstrom, A.; J., C. *Tetrahedron* **1997**, *53*, 6433−6464.

10.1021/ja982995f CCC: $18.00
Published on Web 01/26/1999

complete energy landscape for pentofuranose sugars is critical both for the understanding of the forces which govern these conformational preferences and for the development and evaluation of force field potentials used for molecular mechanics and dynamics simulations.

We have undertaken a systematic study of substituted 5′-dehydroxy pentofuranose sugar analogues to examine the geometries and potential energies of pseudorotation. Initially it was necessary to establish a suitable substitution at C1′ which was computationally feasible and still retained the properties of the full nucleic acid base. Using a pyrrole substitution at C1′, we then identified the level of QM calculation and basis set necessary for accurate geometries (HF/6-31G**) and energies (LMP2/cc-pVTZ), when compared to experimental data. This model cluster (3,4-dihydroxy-5-methyl-2-(1-pyrollyl)tetrahydrofuran for 2′-deoxyribose and 4-hydroxy-5-methyl-2-(1-pyrollyl)tetrahydrofuran for ribose) and gas-phase computational method allowed us to determine the following:

1. For 2′-deoxyribose, the C3′-endo conformation is 0.6 kcal/mol higher in energy than the global minimum C2′-endo conformation and is separated by the 1.6 kcal/mol eastern barrier.

2. For ribose, the C2′-endo conformation remains the global minimum because of the formation of a hydrogen bond between the 3′-OH and 2′-OH, as has been observed by X-ray crystallography.[22,23]

3. Constraining the rotation of the 3′-OH to prevent hydrogen bond formation alters the global minimum to C3′-endo, consistent with the observed sugar pucker preferences of RNA polymers.

In addition, a force field capable of reproducing these ab initio QM results is presented. These new sugar parameters, embedded in the framework of a generic force field, such as UFF,[24] and modified to include our accurate hydrogen bond potential[25] is ideal for molecular mechanics and dynamics simulations of nucleic acids interacting with a diverse collection of organic and inorganic molecules. To begin, it is useful to review some important concepts regarding 2′- and 3′-substituted pentofuranose sugars including pseudorotation, structural nomenclature, anomeric and gauche effects, and previous theoretical work in the field.

Pseudorotation and Structural Nomenclature. Pseudorotation involves the conversion of one ring conformation to another without passing through a high-energy planar state (see Figure 1). Altona and Sundaralingam[26] have derived a simple mathematical relationship relating the five ring torsion angles, $j = 0-4$ (see Figure 2), of pentofuranose to two parameters, τ_m and P.

$$\tau_j = \tau_m \cos(P + 0.8\pi(j - 2)) \qquad (1)$$

τ_m is the maximum pucker amplitude, and P is the pseudorotation phase that may range from 0 to 2π. However, in this work, P is referred to in units of degrees, $0° \le P \le 360°$. Other more complex and rigorous expressions for pseudorotation have been derived.[27] Some require artificial constructs to define the plane $z = 0$ and are useful for systems with unequal bond lengths and angles.[28] A statistical survey of over 100 ribose and deoxyribose crystal structures indicates that τ_m is dependent on both pucker geometry and nature of the sugar.[29] The average τ_m values for 2′-deoxyribose and ribose were found to be 35.2° and 37.1°, respectively.

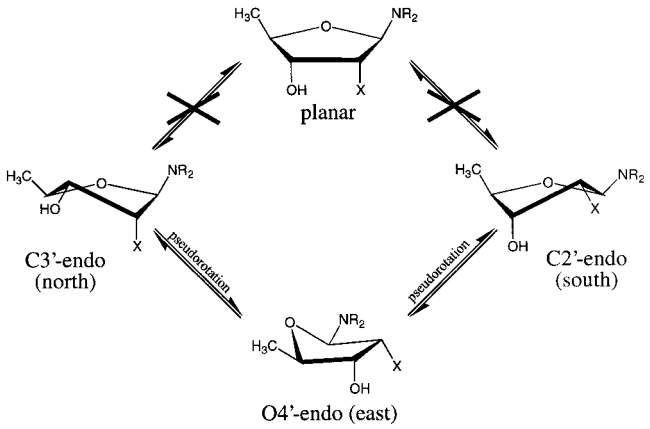

Figure 1. Schematic of the pseudorotation process in which low-energy conformations (C3′-endo and C2′-endo) interconvert without passing through a planar intermediate.

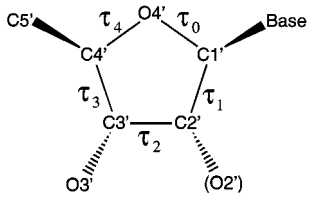

Figure 2. Atom names and torsion definitions for substituted pentofuranose rings. To enforce the pseudorotation pathway, sugar torsion angles τ_0 and τ_4 were constrained as described in the Methods.

In general, there are only two major conformations observed for all ribose and 2′-deoxyribose sugars: C2′-endo and C3′-endo. The 2′ or 3′ designation refers to the atom which is out of the plane of the remaining atoms forming the ring. This atom may lie above the ring plane on the same side as C5′ or on the opposite side, resulting in an "endo" or "exo" conformation, respectively (see Figure 1). Using the pseudorotation phase coordinate P, C3′-endo lies at $P = 18°$ while the C2′-endo conformation is at $P = 162°$. The full pseudorotation cycle also may be divided into quadrants in which conformations clustered around C2′-endo are known as southern or S-type sugars. Similarly, the C3′-endo pucker is a northern or N-type sugar conformation. This nomenclature system is used extensively in the interpretation of NMR experiments in which the measurement of vicinal coupling constants can be used to determine the ratio of N/S sugar conformations.[8−12,15−17,20]

The two energy barriers between the C3′-endo and C2′-endo conformations depend on the direction of pseudorotation: $P = 18° \rightarrow 162°$ via 90° (east) or via 270° (west). Several crystal structures have been reported in which the ring geometry is E-type (O4′-endo), but none have been reported for structures with a W-type (O4′-exo) conformation.[29] Furthermore, NMR experiments indicate a rapid interconversion between the C2′-endo and C3′-endo conformations. On the basis of these observations, it is widely accepted that the western barrier is higher than the eastern barrier, which must be sufficiently low

(22) Murai, Y.; Shiroto, H.; Ishizaki, T.; Iimori, T.; Kodama, Y.; Ohtsuka, Y.; Oishi, T. *Heterocycles* **1992**, *33*, 391−404.
(23) Thewalt, U.; Bugg, C. E.; Marsh, R. E. *Acta Crystallogr., Sect. B* **1970**, *26*, 1089.
(24) Rappé, A. K.; Casewit, C. J.; Colwell, K. S.; Goddard, W. A., III; Skiff, W. M. *J. Am. Chem. Soc.* **1992**, *114*, 10024−10035.
(25) Brameld, K. A.; Dasgupta, S.; Goddard, W. A., III. *J. Phys. Chem. B* **1997**, *101*, 4851−4859.
(26) Altona, C.; Sundaralingam, M. *J. Am. Chem. Soc.* **1972**, *94*, 8205−8221.
(27) Tomimoto, M.; Go, N. *J. Phys. Chem.* **1995**, *99*, 563−577.
(28) Cremer, D.; Pople, J. A. *J. Am. Chem. Soc.* **1975**, *97*, 1354−1358.
(29) Gelbin, A.; Schneider, B.; Clowney, L.; Hsieh, S. H.; Olson, W. K.; Berman, H. M. *J. Am. Chem. Soc.* **1996**, *118*, 519−529.

to allow rapid interconversion at room temperature.[5,30−38] Using ^{13}C NMR relaxation experiments in deuterioammonia, the eastern barrier for purine ribonucleosides is reported to be 4.7 ± 0.5 kcal/mol.[6]

Anomeric and Gauche Effects. The anomeric effect and the gauche effect are two principles that have been invoked to explain the existence and nature of the barriers to pseudorotation for ribose and 2′-deoxyribose. The anomeric effect was first discovered in sugars with the observation that a methoxy group attached to the anomeric carbon prefers the sterically unfavorable axial position.[39] In chemical systems R−X−C−Y, where X has at least one set of lone pair electrons and Y is an electronegative atom, the anomeric effect will favor a gauche torsion angle.[14,17−19,40−44] In that geometry, the lone pair of X may donate into the σ^* antibonding orbital of the C−Y bond. Maximum overlap with the σ^* antibonding orbital occurs when the lone pair is trans to the C−Y bond. For nucleic acids, the anomeric effect arises only for the O4′−C1′−N1(N9)−R and the phosphodiester torsions. It has been suggested that the anomeric effect is critical in defining the eastern barrier during pseudorotation.[40]

Conceptually, the gauche effect is quite similar to the anomeric effect but affects chemical systems of the type X−C−C−Y. Here too electronegative substitutions at X and Y stabilize the gauche conformation relative to the trans conformation.[14,18,19,42,45,46] The gauche effect is important in the ribose and 2′-deoxyribose systems because there are several X−C−C−Y type torsions. For 2′-deoxyribose, these include O4′−C4′−C3′−O3′ and O4′−C4′−C5′−O5′, while ribose has three additional torsions, O4′−C1′−C2′−O2′, N1(N9)−C1′−C2′−O2′, and O2′−C2′−C3′−O3′. These gauche effects result in C2′-endo being the preferred structure for the 2′-deoxyribose sugars found in DNA polymers.

Theoretical Approaches to Pentofuranose Pseudorotation. Early theoretical work using empirically derived potential energy functions gave conflicting results and led to discrepancies between theoretical predictions and experimental observations.[30,47] It was not until the gauche effect was explicitly taken into account that Olson was able to derive an empirical energy function that correlated well with known crystallographic and solution data.[5] Indeed, the potential energies of pseudorotation derived with these functions have been the benchmark against which several popular molecular mechanics/dynamics force fields have been parametrized.[48−52]

Several quantum mechanical studies have been carried out that examine the conformational energies of pentofuranose sugars. Semiempirical and ab initio methods have been used in the pseudorotational analysis of THF.[2,37,53,54] Substituted pentofuranose sugars also have been studied, but in those cases, either the nucleic acid base was not included[14,55] or only the minimum energy conformations were calculated.[56,57] Consequently, the potential energy for pseudorotation of 2′-deoxyribose and ribose systems comparable to those found in natural nucleic acids heretofore had not been determined using ab initio QM methods. The results of a systematic ab initio QM study of substituted pentofuranose sugar analogues are presented herein which addresses this shortcoming.

Methods

Ab Initio Quantum Mechanical Calculations. All ab initio QM calculations were carried out using the Jaguar 3.0 software package.[58] To determine the potential energy of pseudorotation, sugar torsion angles τ_0 and τ_4 (Figure 2) were constrained. Values for τ_0 and τ_4 were calculated using eq 1 and $\tau_0 = 40$. For each point along the pseudorotation pathway, full geometry optimization (HF/6-31G**) was carried out while maintaining the desired τ_0 and τ_4 angles. No restraints were placed upon the glycosidic linkage χ between the sugar and pyrrole. Single-point energies were determined using local second-order Möller−Plesset perturbation theory (LMP2)[59−62] with the cc-pVTZ(-f) basis set[63] and frozen core orbitals. To ensure the points along this constrained pseudorotation pathway were a reasonable approximation of the true pseudorotation pathway, the C3′-endo and C2′-endo conformations were also optimized (HF/6-31G** and LMP2/cc-pVTZ(-f)) with no constraints. In addition, a transition state optimization of O4′-endo conformation (eastern barrier) at the same level with no constraints was also carried out. For some ribose calculations, the C4′−C3′−O3′−H torsion angle was constrained to be −146°, as is found in RNA polymers.[29] This constraint enabled the pseudorotation potential for

(30) Broyde, S.; Wartell, R. M.; Stellman, S. D.; Hingerty, B. *Biopolymers* **1978**, *17*, 1485−1506.
(31) Pearlman, D. A.; Kim, S. H. *J. Biomol. Struct. Dyn.* **1985**, *3*, 99−125.
(32) Harvey, S. C.; Prabhakaran, M. *J. Am. Chem. Soc.* **1986**, *108*, 6128−6136.
(33) Schlick, T.; Peskin, C.; Broyde, S.; Overton, M. *J. Comput. Chem.* **1987**, *8*, 1199−1224.
(34) Gorin, A. A.; Ulyanov, N. B.; Zhurkin, V. B. *Mol. Biol.* **1990**, *24*, 1036−1047.
(35) Gabb, H. A.; Harvey, S. C. *J. Am. Chem. Soc.* **1993**, *115*, 4218−4227.
(36) Rudnicki, W. R.; Lesyng, B.; Harvey, S. C. *Biopolymers* **1994**, *34*, 383−392.
(37) Dobado, J. A.; Molina, J. M.; Espinosa, M. R. *J. Mol. Struct. (THEOCHEM)* **1994**, *109*, 205−212.
(38) Pechenaya, V. I.; Rudnitsky, W.; Gritsuk, T.; Lesyng, B. *Mol. Biol.* **1995**, *29*, 616−627.
(39) Edward, J. T. *Chem. Ind. (London)* **1955**, 1102−1104.
(40) Thatcher, G. R. J. *The Anomeric Effect and Associated Stereoelectronic Effects*; American Chemical Society: Washington, DC, 1993.
(41) Kneisler, J. R.; Allinger, N. L. *J. Comput. Chem.* **1996**, *17*, 757−766.
(42) Murcko, M. A.; Dipaola, R. A. *J. Am. Chem. Soc.* **1992**, *114*, 10010−10018.
(43) Jaffe, R. L.; Smith, G. D.; Yoon, D. Y. *J. Phys. Chem.* **1993**, *97*, 12745−12751.
(44) Juaristi, E.; Cuevas, G. *The Anomeric Effect*; CRC Press: Boca Raton, FL, 1995.
(45) Phillips, L.; Wray, V. *J. Chem. Soc. Chem. Commun.* **1973**, 90−91.
(46) Wiberg, K. B.; Murcko, M. A.; Laidig, K. E.; Macdougall, P. J. *J. Phys. Chem.* **1990**, *94*, 6956−6959.
(47) Warshel, A.; Levitt, M. *J. Am. Chem. Soc.* **1978**, *100*, 2607−2613.
(48) Weiner, S. J.; Kollman, P. A.; Case, D. A.; Singh, U. C.; Ghio, C.; Alagona, G.; Profeta, S.; Weiner, P. *J. Am. Chem. Soc.* **1984**, *106*, 765−784.
(49) Nilsson, L.; Karplus, M. *J. Comput. Chem.* **1986**, *7*, 591−616.
(50) Weiner, S. J.; Kollman, P. A.; Nguyen, D. T.; Case, D. A. *J. Comput. Chem.* **1986**, *7*, 230−252.
(51) Cornell, W. D.; Cieplak, P.; Bayly, C. I.; Gould, I. R.; Merz, K. M.; Ferguson, D. M.; Spellmeyer, D. C.; Fox, T.; Caldwell, J. W.; Kollman, P. A. *J. Am. Chem. Soc.* **1995**, *117*, 5179−5197.
(52) Mackerell, A. D.; Wiorkiewiczkuczera, J.; Karplus, M. *J. Am. Chem. Soc.* **1995**, *117*, 11946−11975.
(53) Cadioli, B.; Gallinella, E.; Coulombeau, C.; Jobic, H.; Berthier, G. *J. Phys. Chem.* **1993**, *97*, 7844−7856.
(54) Strajbl, M.; Baumruk, V.; Florian, J. *J. Phys. Chem. B* **1998**, *102*, 1314−1319.
(55) Serianni, A. S.; Chipman, D. *J. Am. Chem. Soc.* **1987**, *109*, 5297−5303.
(56) Grana, A. M.; Pereiras, A. J.; Rios, M. A. *J. Mol. Stuct. (THEOCHEM)* **1993**, *280*, 211−222.
(57) Orozco, M.; Velasco, D.; Canela, E. I.; Franco, R. *J. Am. Chem. Soc.* **1990**, *112*, 8221−8229.
(58) Ringnalda, M. N.; Langlois, J.-M.; Greeley, B. H.; Murphy, R. B.; Russo, T. V.; Cortis, C.; Muller, R. P.; Marten, B.; Donnelly, R. E.; Mainz, D. T.; Wright, J. R.; Pollard, W. T.; Cao, Y.; Won, Y.; Miller, G. H.; Goddard, W. A., III; Friesner, R. A. *Jaguar 3.0*; Schrödinger, Inc.: Portland, OR, 1997.
(59) Saebo, S.; Pulay, P. *Chem. Phys. Lett.* **1986**, *131*, 384−388.
(60) Saebo, S.; Pulay, P. *J. Chem. Phys.* **1988**, *88*, 1884−1890.
(61) Saebo, S.; Pulay, P. *Annu. Rev. Phys. Chem.* **1993**, *44*, 213−236.
(62) Saebo, S.; Tong, W.; Pulay, P. *J. Chem. Phys.* **1993**, *98*, 2170−2175.
(63) Dunning, T. H. *J. Chem. Phys.* **1989**, *90*, 1007−1023.

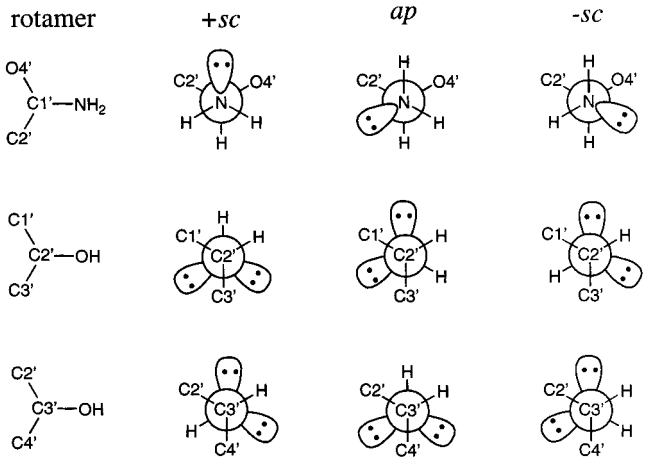

Figure 3. Three possible rotamer conformations for substitutions at C1′, C2′, and C3′.

ribose to be calculated for conformations which were not compromised by an intramolecular hydrogen bond.

Rotamer Definitions. Exocyclic substitutions of an amino group at C1′ or hydroxyl groups at C2′ and C3′ complicate the potential energy surfaces of these sugars. In many cases, the torsion angle about C−N or C−O bond has a considerable impact on the energy of a particular sugar pucker. Figure 3 illustrates the nomenclature which we have adopted to describe each of these rotamers. For the C1′−NH_2 bond, general torsion angles are defined relative to the O4′−C1′ bond and the NH_2 lone pair vector. Thus the +*synclinal* (+*sc*), *antiperiplanar* (*ap*), and −*synclinal* (−*sc*) geometries correspond to (lone-pair)−N−C1′−O4′ torsion angles of 60°, 180°, and −60°, respectively. Similarly, for hydroxyl group substitutions at C2′ and C3′, torsion angles are measured relative to the H−O and C1′−C2′ bonds for substitution at C2′ or the H−O and C3′−C4′ bonds for substitution at C3′. In describing ribose conformational rotamers, the C3′ substitution will be listed first, then the C2′ substitution. For example, a ribose conformation C2′-endo(*ap*/+*sc*) would have an *ap* C3′ hydroxyl group and a +*sc* C2′ hydroxyl group.

Force Field Calculations. The Cerius^2 3.5 software package[64] was used for all molecular mechanics and dynamics simulations. The strategy we employ for force field development begins with a simple generic force field (UFF[24]) which is then tuned to reproduce QM potential energies for small model systems, as has been discussed elsewhere.[65] All standard valence terms including bonds, angles, torsions, and inversions are taken from UFF.[24] The Dreiding FF[66] exponential-6 parameters are used for all van der Waals interactions and a standard Coulombic potential completes the nonbond terms. For pseudorotation of ribose and deoxyribose sugars, two new atom types were required: O_S for O4′ and C_S for C3′. These new atom types allow for the parametrization of several new torsion potentials which take into account anomeric and gauche effects. A standard torsion potential is used and can be represented by a Fourier series of the form

$$E_{\text{torsion}} = \frac{1}{2}\sum_{n=1}^{6} K_{\theta,n}(1 - d\cos(n\phi)) \qquad (2)$$

where $K_{\theta,n}$ is the torsion energy barrier, $d = \pm 1$ and is the phase factor, and ϕ is the torsion angle ($\phi = 0$ for cis). A complete description of the force field atom types and point charges is shown in Figure 4. Atomic point charges were determined from the electrostatic potential derived from the electron density distribution (constrained to reproduce the molecular monopole and dipole moments) calculated from the converged LMP2/cc-pVTZ(-f) wave function.[67] The complete list of force field parameters are included in Tables S1−S5 of the Supporting Information. As is standard with generic force fields such as UFF and Dreiding, the same parameters are used for both molecular dynamics and minimization. Calculations using Amber 4.1[51] and CFF95[68−70] were also carried out in Cerius^2 3.5 and used an $\epsilon = 1$ dielectric constant. Charges and atom types are also included in the Supporting Information (Figure S1).

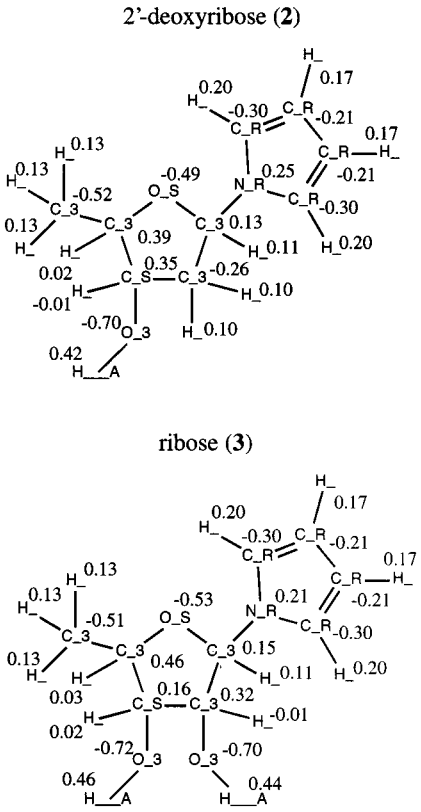

Figure 4. Atomic point charges and MSCFF force field atom types for 2′-deoxyribose and ribose sugar analogues.

Results and Discussion

Model Systems and Level of Theory. A complete potential energy calculation for nucleosides of each naturally occurring base (adenine, thymine, guanine, cytosine, and uracil) is computationally intensive and an alternative sugar model is necessary which still retains the key properties of the full bases. For the first 2′-deoxyribose model system, the full base is substituted with a simple amine (**1**) and a methyl group replaces the 5′-hydroxy methyl group (Scheme 1). Figure 5 shows a plot of the HF/6-31G** relative energies for pseudorotation and the dramatic dependency upon the amine rotamer conformation. The lowest energy pseudorotation path is almost exclusively the *ap* rotamer in which the nitrogen lone pair electrons are trans to the C1′−O4′ bond (see the Methods and Figure 3 for rotamer nomenclature).

Several features of the amine substitution make it unsatisfactory as a model for the aromatic base. In addition to complicating the potential energy surface due to several possible rotamers,

(64) *Cerius^2 3.5*; Molecular Simulations, Inc.: San Diego, CA, 1997.
(65) Dasgupta, S.; Brameld, K. A.; Fan, C. F.; Goddard, W. A., III. *Spectrosc. Chim. Acta A* **1997**, *53*, 1347−1363.
(66) Mayo, S. L.; Olafson, B. D.; Goddard, W. A. *J. Phys. Chem.* **1990**, *94*, 8897−8909.
(67) Tannor, D. J.; Marten, B.; Murphy, R.; Friesner, R. A.; Sitkoff, D.; Nicholls, A.; Ringnalda, M.; Goddard, W. A., III; Honig, B. *J. Am. Chem. Soc.* **1994**, *116*, 11875−11882.
(68) Maple, J. R.; Dinur, U.; Hagler, A. T. *Proc. Natl. Acad. Sci. U.S.A.* **1988**, *85*, 5350−5354.
(69) Dinur, U.; Hagler, A. T. *J. Comput. Chem.* **1990**, *11*, 1234−1246.
(70) Maple, J. R.; Hwang, M. J.; Stockfisch, T. P.; Dinur, U.; Waldman, M.; Ewig, C. S.; Hagler, A. T. *J. Comput. Chem.* **1994**, *15*, 162−182.

Scheme 1. Model Systems Used for All Ab Initio Quantum Mechanical Calculations[a]

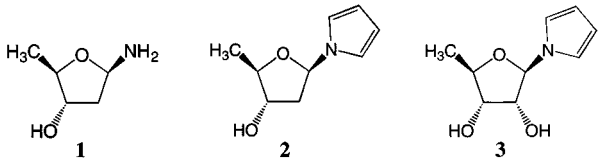

[a] The 2′-deoxyribose models (**1** and **2**) differ by having an amino group or pyrrole group as a substitution for the base at C1′. The ribose (**3**) model has a pyrrole substitution for the base at C1′. Pyrrole-containing models (**2** and **3**) compare well with experimental data and are used to parameterize the MSCFF

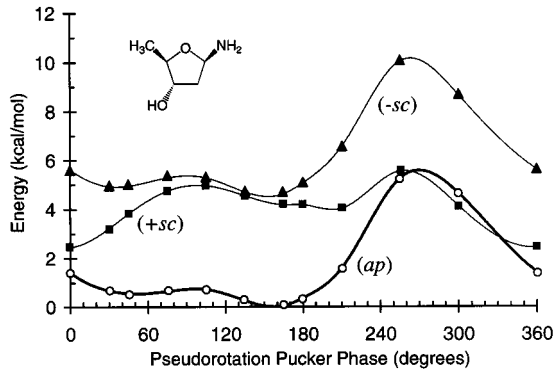

Figure 5. HF/6-31G** potential energy (kcal/mol) for the 2′-deoxyribose analogue (**1**) with an amine substitution for the naturally occurring base as a function of pseudorotation angle *P*. The three possible rotamer conformations for the amino group have very different energies. All energies are reported relative to C2′-endo(*ap*) conformation (−399.925 769 hartree).

the amino group nitrogen has sp^3 hybridization, thereby allowing the lone pair electrons to participate in a strong anomeric effect with O4′. This anomeric effect likely stabilizes the *ap* rotamer relative to ±*sc* rotamers and would not be present for the full base. The lack of an eastern barrier between the C3′-endo and C2′-endo conformations is also problematic and is not consistent with NMR experiments. For these reasons, the amine model was abandoned and a pyrrole substitution, which maintains the aromatic nitrogen, was pursued.

A pyrrole substitution for the complete nucleic acid base is a satisfactory model. The symmetry of the pyrrole ring alleviates complications due to rotamers while simultaneously enforcing sp^2 character on the nitrogen atom. The pseudorotation potential energy curves for a 2′-deoxyribose analogue (**2**) are plotted in Figure 6. The potential energy curve of **2** has a well-defined eastern barrier consistent with NMR data and the expected minima at C2′-endo and C3′-endo.

Several calculations were carried out for the 2′-deoxyribose (**2**) model system to establish the optimum level of computational rigor which yields the best accuracy while still remaining computationally feasible. Table 1 reports the relative energies for complete geometry optimization with no constraints of **2** in the C3′-endo, O4′-endo (eastern barrier), and C2′-endo conformations. The HF/6-31G** and LMP2/cc-pVTZ(-f) optimized geometries are very similar. The only systematic difference observed between the two levels of theory is the C4′−O4′−C1′ angle which averages 2.5° less for the LMP2/cc-pVTZ(-f) optimized structures. Given the small structural difference between these two methods, all subsequent geometry optimizations were carried out at the HF/6-31G** level, followed by LMP2/cc-pVTZ(-f) single-point energies.

2′-Deoxyribose Analogue. The HF/6-31G** and LMP2/cc-pVTZ(-f) pseudorotation potential energies are plotted in Figure

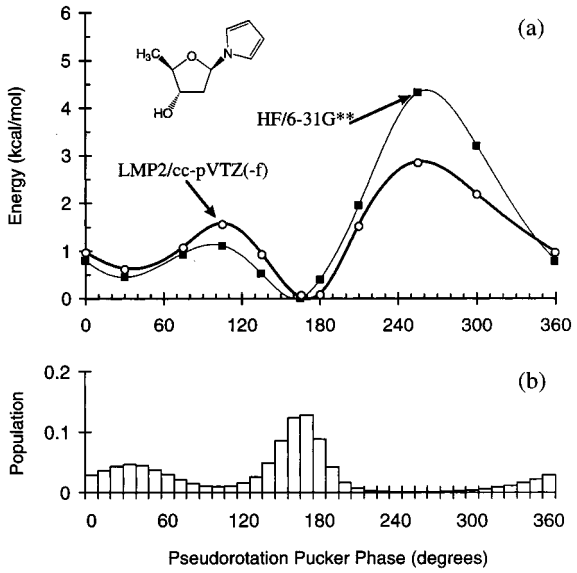

Figure 6. (a) HF/6-31G** and LMP2/cc-pVTZ(-f) potential energies (kcal/mol) as a function of pseudorotation angle *P* for the 2′-deoxyribose analogue (**2**) with a pyrrole substitution for the naturally occurring base. All energies are reported relative to the C2′-endo conformation (HF/6-31G** = −552.548 378; LMP2/cc-pVTZ(-f) = −554.634 699 hartree). (b) Normalized statistical weights σ at $T = 298$ K using the LMP2/cc-pVTZ(-f) energies.

Table 1. Relative Energies (kcal/mol) for the Fully Optimized 2′-Deoxyribose Analogue (**2**)

method	C3′-endo	O4′-endo	C2′-endo
HF/6-31G**//HF/6-31G**	0.44	1.16	0.00[a]
LMP2/cc-pVTZ(-f)//HF/6-31G**	0.40	1.31	0.00[b]
LMP2/cc-pVTZ(-f)//LMP2/cc-pVTZ(-f)	0.61	1.19	0.00[c]

[a] Absolute energy = −552.548 294 hartree. [b] Absolute energy = −554.634 699 hartree. [c] Absolute energy = −554.636 953 hartree.

6a. Both curves have the same general trend with a global minimum C2′-endo conformation. The C3′-endo conformation is 0.6 and 0.4 kcal/mol higher in energy for the LMP2/cc-pVTZ(-f) and HF/6-31G** curves, respectively. The O4′-endo barrier is well defined with maximum energies of 1.6 and 1.1 kcal/mol for the LMP2/cc-pVTZ(-f) and HF/6-31G** curves, respectively. There is excellent agreement between the fully optimized HF/6-31G** points listed in Table 1 and the constrained pseudorotation curve in Figure 6a. This indicates that the torsion constraints used for the pseudorotation calculations are a reasonable representation of the true pseudorotation pathway.

For all of the calculations presented above, the 3′-hydroxyl group is in a −*sc* rotamer conformation. Examination of all three possible hydroxyl group orientations for the C2′-endo conformation indicated that the *ap* and −*sc* orientations are essentially degenerate. The HF/6-31G** energies are 1.34, 0.00, and 0.01 kcal/mol for +*sc*, *ap*, and −*sc*, respectively. Including electron correlation (LMP2/cc-pVTZ(-f)) changes these energies slightly to 1.34, 0.01, and 0.00 kcal/mol for +*sc*, *ap*, and −*sc* respectively. Because the −*sc* conformation is the (LMP2/cc-pVTZ(-f)) global minimum, this conformation was chosen for the full-potential surface analysis. In a DNA polymer, the torsion angle formed by the phosphate, which replaces the hydrogen of the hydroxyl group, lies between the −*sc* and *ap* rotamers. Thus these calculations indicate that the conformation of this torsion angle does not strongly affect pseudorotation energies.

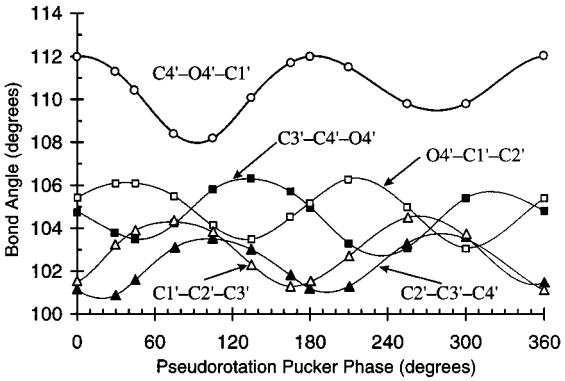

Figure 7. Endocyclic bond angles for the 2′-deoxyribose analogue (**2**) as a function of pseudorotation angle *P*. There is a strong coupling between the pseudorotational phase and all the bond angles.

An analysis of the endocyclic bond angles of the furanose ring reveals a strong correlation between pseudorotational phase and bond angles (Figure 7). This correlation is observed experimentally[29] and is predicted from pseudorotation theory.[1,7,27] Endocyclic bond angles for which the central atom is C1′, C2′, C3′, or C4′ all oscillate in the range 101°−106° and are fairly symmetrical. In contrast, the C4′−O4′−C1′ bond angle oscillates in the range 108°−112° and is noticeable unsymmetrical. For the O4′-exo conformations found near $P = 270°$, steric interactions between the C4′ and C1′ substituents force the C4′−O4′−C1′ bond angle to increase and that portion of the curve to be unsymmetrical when compared to the O4′-endo conformation. The resulting angle strain, in combination with van der Waals interactions, leads to a high western barrier.

The statistical populations ($T = 298$ K) of **2** are plotted versus pseudorotation phase in Figure 6b. These populations are derived from the LMP2/cc-pVTZ(-f) single-point energies and are normalized by the total energy of the system. Summing each of these contributions into quadrant populations gives the following: $\sigma_n = 0.26$, $\sigma_e = 0.18$, $\sigma_s = 0.54$, $\sigma_w = 0.02$. As expected from crystallographic studies, the σ_s quadrant is heavily favored. These populations are different from those reported by Olson using an empirically derived potential energy function.[5] The empirical potential energy function overestimates σ_s ($\sigma_s = 0.74$) and predicts σ_n and σ_e to be almost equal. A study of 127 mononucleoside and mononucelotide crystal structures[29] reported 78 C2′-endo conformations ($\sigma_s = 0.61$), 31 C3′-endo conformations ($\sigma_n = 0.24$), and 18 conformations ($\sigma_e = 0.14$) which were neither C2′-endo nor C3′-endo and presumably in the O4′-endo range. Thus the LMP2/cc-pVTZ(-f) potential energies are in excellent agreement with available crystallographic data.

Using NMR, it is difficult to quantify the energy barrier between low-energy conformations. However, NMR experiments which measure vicinal coupling constants can be used to determine σ_n and σ_s. A study measuring σ_s of five 2′-deoxyribose nucleosides (dA, dG, dC, dT, and dU) at 278 and 358 K has been reported.[19] An average over the five different bases gives mean experimental values for σ_s of 0.66 and 0.62 at the two temperatures, respectively. Summing the QM energy derived populations into hemispheres (NMR experiments resolve the sugar conformations only into N-type or S-type) at 278 and 358 K gives $\sigma_s = 0.64$ and $\sigma_s = 0.59$, consistent with the NMR experiments. The remarkable correlation of ab initio QM results with both crystallographic and NMR data suggests that both our model system containing a pyrrole and the LMP2/cc-pVTZ(-f)//HF/6-31G** potential energies give an accurate representation of 2′-deoxyribose pseudorotation.

Table 2. HF/6-31G** Relative Energies for All Nine Possible Rotamers for the Ribose Analogue (**3**) in Both the C3′-endo and C2′-endo Optimum Conformations

rotamer	−*sc* (C3)	ap (C3)	+*sc* (C3)
	C3′-endo		
−*sc* (C2)	n/m[b]	n/m	3.14
ap (C2)	1.14	0.98	1.38
+*sc* (C2)	6.48	n/m	0.92
	C2′-endo		
−*sc* (C2)	2.03	2.60	3.88
ap (C2)	n/m	n/m	n/m
+*sc* (C2)	5.23	**0.00**[a]	n/m

[a] Absolute energy = −627.407 965 hartree. [b] n/m indicates that this conformation is not a local energy minimum and geometry optimization leads to a neighboring minimum conformation listed in this table.

Ribose Analogue. Applying the same computational methods established for the 2′-deoxyribose model (**2**) to determine the pseudorotation potential of the ribose model (**3**) is considerably more complex due to the multiple possible conformations of the 2′- and 3′-hydroxyl groups. Each hydroxyl group may assume one of three possible orientations, +*sc*, −*sc*, and *ap*, giving a total of nine distinct rotamer combinations for each pucker state. Some of these rotamer combinations are sterically forbidden and most are energetically unfavorable. To identify those rotamers which are most likely sampled during pseudorotation, all nine possible rotamers in both the C3′-endo and C2′-endo sugar conformations were geometry optimized (HF/6-31G**). No constraints were used to enforce the rotamer geometry; therefore, some conformations did not yield minimized structures. Table 2 reports the energies of those conformations which did constitute local minima. Interestingly, the lowest energy conformations are C2′-endo(*ap*/+*sc*) and C3′-endo(+*sc*/+*sc*), both sharing the +*sc* rotamer at the C2′ hydroxyl group.

Pseudorotation potential energies were calculated for the ribose analogue (**2**) in both the (*ap*/+*sc*) and (+*sc*/+*sc*) rotamer conformations. As expected, both rotamers are required to map the lowest energy pseudorotation pathway for ribose as shown in Figure 8a. The interconversion between the two rotamer conformations occurs at the eastern (O4′-endo) and western (O4′-exo) barriers. The (*ap*/+*sc*) conformation is favorable in the northern hemisphere ($P = 270°-360°$; $0°-90°$) while the (+*sc*/+*sc*) conformation is preferred in the southern hemisphere ($P = 90°-270°$). Single-point energies (LMP2/cc-pVTZ(-f)) were calculated only for the lowest energy rotamer at each point. Perhaps the most surprising result is that the C2′-endo conformation remains the global minimum for ribose. The C3′-endo conformation lies 0.6 kcal/mol higher in energy with an eastern barrier of 1.8 kcal/mol separating the two minima. These energies are unexpected given the known preference for RNA polymers to assume an A-form helix which requires the C3′-endo sugar conformation.

NMR studies of ribonucleosides reveal that the nature of the base has a marked influence upon the preferred sugar pucker. Purine bases A and G have σ_s populations of 0.70 and 0.67, respectively, at $T = 278$ K. However, pyrimidine bases C, T, and U have a greater preference for the C3′-endo pucker with σ_s populations of 0.35, 0.49, and 0.46.[19] Using the LMP2/cc-pVTZ(-f) single point energies, the predicted populations of **3** are shown in Figure 8b. Due to the slight broadening of the C2′-endo potential energy minimum and an increase in the eastern barrier height when compared to 2′-deoxyribose, σ_s for ribose increases to 0.70, in agreement with the purine ribonucleoside NMR data. The unique behavior of the pyrimidine ribonucleosides is not predicted by the pyrrole model. Perhaps

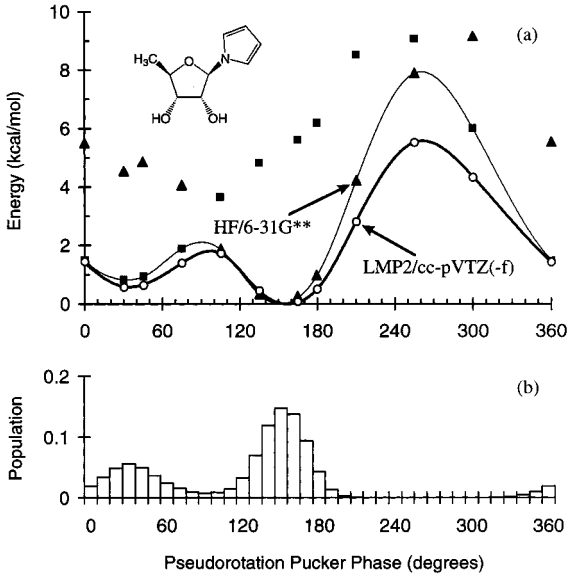

Figure 8. (a) HF/6-31G** and LMP2/cc-pVTZ(-f) potential energies (kcal/mol) as a function of pseudorotation angle *P* for the ribose analogue (**3**) with a pyrrole substitution for the naturally occurring base. For the HF/6-31G** points, two possible C3′ rotamers were examined: (▲) = *ap*/+*sc*; (■) = +*sc*/+*sc*. It is clear that both rotamers are needed to trace out the lowest energy path shown. LMP2/cc-pVTZ(-f) energies are calculated only for the most favorable rotamer. All energies are reported relative to the C2′-endo(*ap*/+*sc*) conformation (HF/6-31G** = −627.407 468; LMP2/cc-pVTZ(-f) = −629.725 164 hartree). (b) Normalized statistical weights σ at $T = 298$ K using the LMP2/cc-pVTZ(-f) energies.

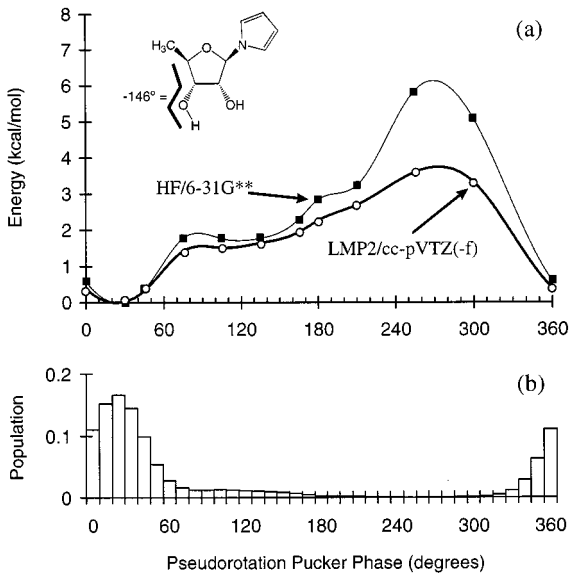

Figure 9. (a) HF/6-31G** and LMP2/cc-pVTZ(-f) potential energies (kcal/mol) as a function of pseudorotation angle *P* for the ribose analogue (**3**) but with the C4′−C3′−O3′−H torsion angle constrained to −146°. This geometric constraint mimics the properties of RNA polymers. All energies are reported relative to the C3′-endo conformation (HF/6-31G** = −627.406 345; LMP2/cc-pVTZ(-f) = −629.72 4598). (b) Normalized statistical weights σ at $T = 298$ K using the LMP2/cc-pVTZ(-f) energies.

these compounds assume nonstandard base geometries which exert an altered electronic influence on the furanose ring. There is evidence from ^{13}C NMR relaxation experiments that pyrimidine ribonucleosides form a hydrogen bond between the 5′-hydroxymethyl group and the base which is not possible in the ribose model (**3**).[6]

A closer examination of the global minimum C2′-endo(*ap*/+*sc*) conformation of the ribose analogue (**3**) suggests that a likely explanation for the unusual stability of this conformation stems from an intramolecular hydrogen bond between the C3′ hydroxyl hydrogen and C2′ hydroxyl oxygen atoms. Experimentally, an intramolecular hydrogen bond has been observed for several ribose crystal structures and does lead to a C2′-endo sugar conformation.[22,23] The presence of this intramolecular hydrogen bond compromises the ribose sugar analogue (**3**) as a model for a ribose polymer or for comparison to experimental studies in aqueous solution. In the first case of a ribose polymer, the C3′ hydroxyl hydrogen atom is not present, having been replaced by a phosphate group, and thus cannot form the hydrogen bond in question. Second, in solution, such intramolecular hydrogen bonds are largely replaced by solvent interactions and are overestimated in gas-phase calculations.[71,72] To better understand ribose sugar behavior in RNA polymers and for the purpose of force field development, it is desirable to design a model system which is not encumbered by an intramolecular hydrogen bond.

Constrained 3′-OH Ribose Analogue. One method to eliminate the hydrogen bond donor properties of the C3′ hydroxyl group is by constraining the C4′−C3′−O3′−H torsion angle to −146°, the same average position assumed by a phosphate atom in dinucleoside monophosphate and trinucleoside diphosphate crystals.[29] The resulting pseudorotation potential for ribose with a constrained C3′ hydroxyl group is shown in Figure 9a. Now, the C3′-endo conformation is the global minimum. Indeed, there is little or no local minimum corresponding to C2′-endo and it is clear why RNA polymers assume a C3′-endo sugar pucker. An analysis of the relative populations of N-type and S-type sugars indicates an overwhelming preference for the northern hemisphere ($\sigma_n = 0.90$).

There is experimental data which supports a strong correlation between the C3′−O3′ torsion angle and ribose sugar pucker. NMR studies of ribodinucleoside monophosphates indicate a C3′-endo ↔ C2′-endo equilibrium with a bias toward the C3′-endo pucker. Furthermore, the C3′-endo pucker is associated with an *ap* torsion angle while the C2′-endo pucker is present with a −*sc* torsion angle.[73] This NMR data is consistent with the constrained pseudorotation potential for ribose which has a C3′-endo global minimum for the *ap* conformation.

While a DNA duplex may undergo a transition from a B-form helix (C2′-endo) to an A-form (C3′-endo) helix with changes in the aqueous environment, RNA polymers do not experience an analogous transition and remain in an A-form conformation. Various explanations based upon the presence of the C2′-hydroxyl group have been put forth to account for the structural stability of RNA polymers.[3] Intramolecular stabilization through hydrogen bonding between O2′−H and O4′ of the neighboring sugar[74] or a water-mediated hydrogen bond between O2′−H and 3′-phosphate[75,76] have been proposed based on NMR data. Alternative rationalizations include electronic effects due to the

(71) Nagy, P. I.; Durant, G. J.; Smith, D. A. *Modeling the Hydrogen Bond* **1994**, *569*, 60−79.
(72) Shan, S. O.; Herschlag, D. *Proc. Natl. Acad. Sci. U.S.A.* **1996**, *93*, 14474−14479.
(73) Sarma, R. H. *Nucleic Acid Geometry and Dynamics*; Pergamon Press: New York, 1980.
(74) Young, P. R.; Kallenbach, N. R. *J. Mol. Biol.* **1978**, *126*, 467−479.
(75) Bolton, P. H.; Kearns, D. R. *Biochim. Biophys. Acta* **1978**, *517*, 329−337.
(76) Bolton, P. H.; Kearns, D. R. *J. Am. Chem. Soc.* **1979**, *101*, 479−484.

Table 3. Relative Energies (kcal/mol) for Pseudorotation of Tetrahydrofuran (THF)

P	HF/6-31G**	MSCFF
0	0.00[a]	0.00[b]
30	0.15	0.14
60	0.37	0.32
90	0.44	0.48

[a] Absolute energy = −230.988 771 hartree. [b] Absolute energy = 15.62 kcal/mol.

preference for a C3′-endo pucker with increasing electronegativity of the C2′ substituent[77] or unfavorable steric interactions which preclude other sugar conformations. Our calculations indicate that no intramolecular hydrogen bond with a neighboring nucleotide or with a bridging water molecule is required to induce a preference for a C3′-endo pucker. The combined electronic effects of the 2′-hydroxyl group and the constrained orientation of the C3′−O3′ torsion angle are sufficient to drive the pseudorotation potential of ribose sugars in RNA polymers completely to the A-form or C3′-endo pucker.

Force Field Development. Using the potential energies for pseudorotation of 2′-deoxyribose and ribose sugar analogues presented above, a set of force field (FF) parameters have been developed for accurate molecular mechanics and dynamics simulations of 2′-deoxyribose- or ribose-containing systems. All standard valence terms including bonds, angles, torsions, and inversions are taken from UFF.[24] The Dreiding FF[66] exponential-6 parameters are used for all van der Waals interactions and a standard Coulombic potential completes the nonbond terms. Upon the framework of this generic FF, two atom types unique to pentofuranose sugars are defined; C_S and O_S for C3′ and O4′, respectively. These atom types allow for the explicit parametrization of anomeric and gauche effects necessary to reproduce QM potential energies. A complete listing of FF parameters is included in Tables S1−S5 of the Supporting Information.

Only two additional torsion types are needed to reproduce the pseudorotation potentials of 2′-deoxyribose and ribose (unconstrained and constrained 3′-hydroxyl group) sugars. The first torsion potential accounts for the gauche preference of O_S−C_3−C_S−C_3 by adding a 2-fold term to the existing C−C 3-fold potential. Table 3 reports the QM and FF pseudorotation energies for tetrahydrofuran which serves as the model system for this generic X−C−C−C torsion. The second new potential applies to all O_x−C_x−C_x−(O_x or N_R) torsions, where $x = 3$ or S types. In practice, this accounts for all torsions of the type X−C−C−Y, in which X and Y are electronegative atoms. It is common for these types of torsions to be parametrized with a combination of 2-fold and 3-fold potentials.[5,48,50−52] Surprisingly, we find it is not possible to reproduce the QM potential energies using only 2-fold and 3-fold potentials for X−C−C−Y type torsions. This type of potential results in local minima located at $P = 0°$ and 180°, not the desired $P = 30°$ and 165°. The use of a 2-fold, 3-fold, and 4-fold potential is capable of reproducing the QM potential energies. The same torsion barriers are used for all atom types, and the resulting FF accurately reproduces the pseudorotation potentials of both ribose and 2′-deoxyribose sugars.

Force Field Evaluation. Figure 10 plots the pseudorotation potential energies calculated with the MSCFF for 2′-deoxyribose and ribose sugars. The position and energies for the two minima at C3′-endo and C2′-endo are well described, as is the eastern O4′-endo barrier. In some cases, the western barrier is overestimated as a result of steric interactions between C5′ and the pyrrole base. The FF has a higher penalty for deformation of the pyrrole ring to relieve these steric clashes than is calculated by QM methods. These regions of the potential energy surface will not be populated during typical MD simulations, and thus the resulting errors will be negligible.

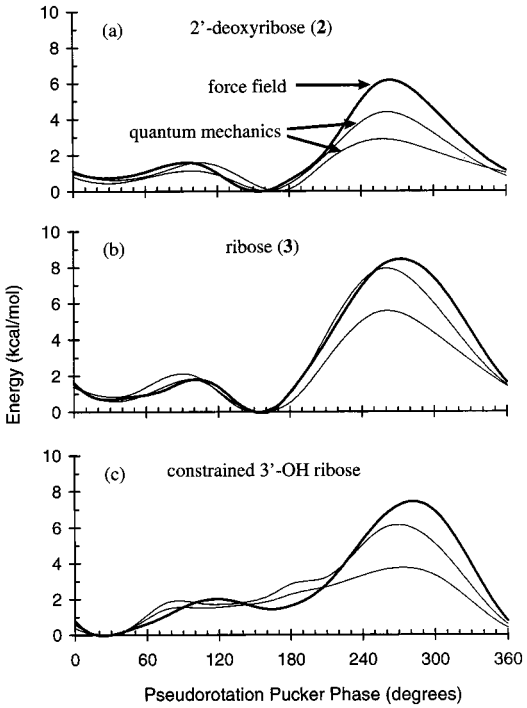

Figure 10. MSCFF potential energies for analogues of (a) 2′-deoxyribose, (b) ribose, and (c) ribose with a constrained C3′-hydroxyl group. The heavy lines are the force field energies, while the lighter lines are HF/6-31G** and LMP2/cc-pVTZ(-f) energies (plotted in detail in Figures 6a, 8a, and 9a).

Table 4. Statistical Weights for the North, East, South, and West Quadrants of Pseudorotation Phase as Determined from Potential Energy Calculations

method	σ_n	σ_e	σ_s	σ_w
2′-Deoxyribose Analogue (**2**)				
LMP2/cc-pVTZ(-f)// HF/6-31G**	0.26	0.18	0.54	0.02
MSCFF	0.18	0.19	0.63	0.00
Amber 4.1	0.13	0.21	0.66	0.00
CFF95	0.76	0.16	0.08	0.00
Ribose Analogue (**3**)				
LMP2/cc-pVTZ(-f)// HF/6-31G**	0.22	0.21	0.58	0.00
MSCFF	0.18	0.19	0.63	0.00
Amber 4.1	0.59	0.24	0.17	0.01
CFF95	0.05	0.06	0.89	0.00
Constrained 3′-OH Ribose Analogue				
LMP2/cc-pVTZ(-f)// HF/6-31G**	0.79	0.17	0.04	0.01
MSCFF	0.66	0.27	0.07	0.00
Amber 4.1	0.83	0.16	0.00	0.01
CFF95	0.96	0.03	0.02	0.00

Table 4 compares the quadrant populations at $T = 298$ K for the LMP2/cc-pVTZ(-f) energies and several force fields including MSCFF, Amber 4.1,[51] and CFF95.[70] The MSCFF populations are in good agreement with the QM predictions for all three cases examined. Amber 4.1 is biased toward C2′-endo conformation for 2′-deoxyribose and C3′-endo for ribose sugars. This bias is expected, as the Amber 4.1 FF is intended for simulations of canonical DNA or RNA polymers. However, the resulting simulations may reflect an unrealistic stability for

(77) Uesugi, S.; Miki, H.; Ikehara, M.; Iwahashi, H.; Kyogoku, Y. *Tetrahedron Lett.* **1979**, *42*, 4073−4076.

B-form DNA and A-form RNA. CFF95 does not reproduce the populations of 2′-deoxyribose and ribose sugars correctly. Indeed, C3′-endo is the preferred conformation for 2′-deoxyribose while C2′-endo is preferred for ribose, in complete contradiction to the QM predictions.

Conclusions

The pseudorotation potential energy calculations presented here provide an updated estimate of the local minima and energy barriers associated with the conformations of 2′-deoxyribose and ribose sugars. Although the model systems employed in these ab initio QM calculations lack a 5′-hydroxyl group, the predicted energies are in good agreement with available NMR and crystallographic data. It is intriguing to note that the lack of a solvation description in these calculations is not evident when compared to experimental results. It may be argued that a crystallographic environment is sufficiently anhydrous to minimize the differences with gas-phase calculations. However, the predicted σ_s and σ_n populations also agree well with NMR studies that are in aqueous solution. One possible explanation for these results is that the effects of solvation on conformation are subtle and are not within the resolution of NMR experiments that coarsely define pseudorotation phase in terms of hemispheres. However, it cannot be ruled out that, for systems containing a phosphate group, solvent effects in conjunction with a modified electrostatic environment may alter the pseudorotation potential energy surface.

The pseudorotation potential energies reported in this work are in qualitative agreement with the benchmark empirical potential derived by Olson on the basis of experimental data.[5,7] However, the Olson potential overestimates the ribose eastern barrier and does not correctly describe the positions of the local minima; a shortcoming consistent with the use of only a 2-fold and 3-fold torsion potential to represent the gauche effect. Because the parametrization of many force fields for nucleic acids are based upon the Olson potential, these new QM potential energies are significant for the evaluation of current force fields and the development of second-generation potentials.

Here it is demonstrated that the complex energy potential of pseudorotation may be accurately determined using high-level quantum mechanical calculations. Furthermore, as detailed simulations of nucleic acids including explicit solvent become more common, it is increasingly critical that the force fields used reflect an accurate potential energy surface, not just the global minimum. These ab initio calculations and the MSCFF are part of a continuing effort to parametrize biological force fields from first principles. The final goal is a new generation force field containing relatively simple functions which are parametrized independently from experimental observations.

Acknowledgment. This research was funded initially by DOE-BCTR (DE-FG36-93CH105 81, David Boron) and finished under support from the NSF (CHE 95-22179) and NIH (EY 11759-01). The facilities of the MSC are also supported by grants from the NSF (ASC 92-100368), Chevron Petroleum Technology Co., BP Chemical, Beckman Institute, Asahi Chemical, Owens-Corning, Exxon, Chevron Chemical Co., Chevron Research and Technology Co., and Avery-Dennison. K.A.B. acknowledges an NIH Predoctoral Biotechnology Training Grant.

Supporting Information Available: Complete set of MSCFF parameters (Tables S1−S5) and atomic charges and atom types for simulations with Amber 4.1 and CFF95 (Figure S1) (PDF). This material is available free of charge via the Internet at http://pubs.acs.org.

JA982995F